

Statistical modeling of groundwater geochemistry in northeastern Brazil

José Francisco de Francisco Oliveira Júnior (✉ junior_inpe@hotmail.com)

Federal University of Alagoas <https://orcid.org/0000-0002-6131-7605>

Alex Souza Moraes

Universidade Federal Rural de Pernambuco

Héliton Pandorfi

Universidade Federal Rural de Pernambuco

Jhon Lennon Bezerra da Silva

Universidade Federal Rural de Pernambuco

Pedro Henrique Dias Batista

Universidade Federal Rural de Pernambuco

Alexandre Maniçoba Rosa Ferraz Jardim

Universidade Federal Rural de Pernambuco

Gledson Luiz Pontes de Almeida

Universidade Federal Rural de Pernambuco

Taize Calvacante Santana

Universidade Federal Rural de Pernambuco

Marcio Mesquita

Universidade Federal Rural de Pernambuco

Research Article

Keywords: mineral water, Beberibe aquifer, geostatistics, water quality

Posted Date: February 11th, 2022

DOI: <https://doi.org/10.21203/rs.3.rs-1210837/v1>

License:   This work is licensed under a Creative Commons Attribution 4.0 International License.

[Read Full License](#)

Abstract

The objective is to characterize the hydrochemical and qualitative composition of the groundwater of the Beberibe aquifer located in the Northeast of Brazil (NEB) using geostatistical, geoprocessing, and multivariate analysis techniques. The Beberibe aquifer is located in the state of Pernambuco (PE), NEB, and is responsible for supplying water to the northern portion of the Recife Metropolitan Region (RMRE). The data collected came from 34 georeferenced mining and mineral water production units. From this, a Piper diagram was constructed and hydrogeological and hydrochemical spatial maps were generated. The data were submitted to descriptive statistics, geostatistics, and principal component analysis (PCA). The results showed that the artesian wells near the coast have a porous geological formation. In all artesian wells, the waters are of the mixed bicarbonate type and highly potable for human consumption. The coefficient of variation was medium to high for all hydrochemical variables. The variables showed a better fit to the Gaussian model, in the study of spatial dependence. In PCA, Cl was the one with the highest correlation with nitrate (NO_3). The anthropogenic influence on water quality at the center of RMRE, mainly on NO_3 concentrations, had a direct impact on water quality for human health.

1. Introduction

Brazil has the largest freshwater reservoir in the world, equivalent to 14% of the total planet Earth, being a country of high relevance worldwide in the supply of mineral water (Tundisi, 2008; Kunrath et al., 2020). In recent years, bottled mineral water has grown significantly on a national scale and thus has become an attractive and profitable business in Brazil (DNPM, 2016; ABINAM, 2020). The worldwide consumption of mineral water reached 284.1 billion liters in 2016, while other beverages, for example, soft drinks reached 159.1 billion liters in the same period (Huang and Liu, 2017), due to these increases, the need for evaluations and analyzes of the quality of drinking water becomes essential and with high frequency (Shruti et al., 2020).

The consumer bases his choice on extrinsic factors, such as brand and personal habits (Pacheco et al., 2018). Mineral waters are products differentiated by intrinsic factors, mainly by their aroma and flavor, which are classified according to the hydrochemical parameters that, in turn, result from the characteristics of the rocks and the aquifer (depth of the water table, as for circulation, confinement, and porosity) that the water flows until its capture and packaging (Dias and Bernardes, 2016; Guadayol et al., 2016; Pacheco et al., 2018).

The quality of mineral water is highlighted by Nunes et al. (2018), who showed the importance of its determination, in which, the hydrochemical composition is the qualitative aspect of greatest importance to be investigated since it has a direct impact on human health. Bulia and Enzweiler (2018) evaluated the bottled water taken from 78 different sources in the state of São Paulo, Brazil, and found that the hydrochemical composition, in general, satisfactorily represented the groundwater in the aquifers corresponding to the bottled mineral water samples. Schwanz et al. (2016), highlighted the potential of

concentrations of perfluorooctanoic acid (PFOA) classified in Group 2B (i.e., the possible presence of a carcinogen for humans), of bottled mineral water in Brazil.

The statistical representation of the hydrochemical composition of mineral water is relatively representative. However, the complementary analysis of the spatial variability allows a careful assessment when investigating the distribution of mineral water in the regions and, thus, makes it possible to question the intrinsic and extrinsic factors that alter the hydrochemical composition of these waters.

Studies like Gilabert-Alarcón et al. (2018), who evaluated the processes that affect the quality of groundwater, using hydrochemical tracers, as the main ionic composition and stable isotopes of water and nitrates, through the synthetic pollution index, allowed the spatial regionalization of groundwater quality. Concomitant with the use of geostatistical techniques that present satisfactory recent results in the spatialization of the hydrochemical composition of groundwater (Jang, 2015; Gu et al., 2017; Arshad et al., 2019; Bodrud-Doza et al., 2019).

Bulia and Enzweiler (2018), highlighted that the groundwater sampling method based on bottled mineral water is a low-cost and viable alternative for determining the composition and hydrochemical quality of the water, without logistical and bureaucratic limitations with conventional sampling (laboratory) on a continental scale.

Because of the above, the study aims to characterize the hydrochemical and qualitative composition of the groundwater of the Beberibe aquifer located in Northeastern Brazil via geostatistical, geoprocessing, and multivariate analysis techniques.

2. Material And Methods

2.1. Location and characterization of the study area

The study was realized in the municipalities of Recife, Olinda, Paulista, São Lourenço da Mata, Camaragibe, and Paudalho, both municipalities are located in the state of Pernambuco (PE), Northeastern Brazil (NEB) (Figure 1). The municipality of Paudalho is located in the mesoregion of Zona da Mata, while Recife, Olinda, Paulista, São Lourenço da Mata, and Camaragibe are located in the mesoregion Metropolitana de Recife, the municipalities are located between the parallels 7°51'0.0" S – 8°8'0.0" S and between the meridians 35°11'0.0" W – 34°54'0.0" W. According to the Köppen-Geiger climate classification, the study region is in two climatic zones: "Am" —humid or sub-humid tropical climate and "Aw" —tropical climate with a dry winter season (Figure 1) - (Beck et al., 2018).

[INSERT TO FIGURE 1 HERE]

The research was conducted in the Beberibe aquifer, the main aquifer that supplies the northern part of the Metropolitan Region of Recife (RMRE), having been explored for over fifty years (CPRH, 2020). In the last decade, with the significant increase in the number of artesian wells, as well as the increase in industrial

activities implemented, followed by population densification and the urbanization process, among others, there was a need to assess the quality of groundwater (CPRH, 2020).

RMRE is located on a Deltaic Plain, which has distinct hydrogeological characteristics, composed of sediments of different origins: fluvial, marine, colluvial, and mangroves, which cover the coastal sedimentary basins of Pernambuco and Paraíba, respectively to the south and north of the region, separated by the structural divider Lineamento Pernambuco. Figure 2 illustrates the spatial distribution of hypsometry, to establish a detailed understanding of the Beberibe aquifer that contemplates the western portion of the Pernambuco coast, with a variation from 0 (coast of the state of Pernambuco) to 261 m of altitude.

[INSERT TO FIGURE 2 HERE]

2.2. Data collect

The in-situ data collection was carried out in 34 extraction units (i.e., artesian wells) that capture mineral water, georeferenced, based on the analyzes made available by the companies and following the rules of the Pernambuco Health Surveillance Agency (APEVISA, 2020). The representation of the spatial distribution of artesian wells is shown in Figure 1.

The record of the hydrochemical values were those made available on the label of each mineral water unit, according to electrical conductivity (EC, $\mu\text{S. Cm}^{-1}$), hardness (Hn, $\text{mg. L}^{-1} \text{CaCO}_3$), hydrogen potential (pH, dimensionless), evaporative resistance (DR, mg. L^{-1}), calcium (Ca, mg. L^{-1}), magnesium (Mg, mg. L^{-1}), sodium (Na, mg. L^{-1}), potassium (K, mg. L^{-1}), bicarbonate (HCO_3 , mg. L^{-1}), sulfate (SO_4 , mg. L^{-1}), chlorine (Cl, mg. L^{-1}), iron (Fe, mg. L^{-1}), manganese (Mn, mg. L^{-1}), fluorine (F, mg. L^{-1}), silicon (Si, mg. L^{-1}), nitrate (NO_3 , mg. L^{-1}), strontium (Sr, mg. L^{-1}), zinc (Zn, mg. L^{-1}) and barium (Ba, mg. L^{-1}).

Table 1 shows the maximum permitted values (MPVs) of the hydrochemical parameters of mineral water for human consumption, according to the Ministry of Health, Ordinance n°. 26, of January 15, 1999, and of the Environmental Company of the State of São Paulo (CETESB) – (Ministério da Saúde, 1999; Ministério da Saúde, 2006; CETESB, 2016).

Table 1

Hydrochemical parameters of water for human consumption and their maximum allowed values (MPVs) according to Brazilian legislation.

| Parameters | Unit | MPV | Parameters | Unit | MPV |
|---|---------------------|--------|--------------------------------|---------------------------------------|-----|
| ¹ NO ₃ | mg. L ⁻¹ | 10 | ¹¹ F | mg. L ⁻¹ | 1.5 |
| ² DR | mg. L ⁻¹ | 1000 | ¹² Zn | mg. L ⁻¹ | 5 |
| ³ pH | - | 6 to 9 | ¹³ Fe | mg. L ⁻¹ | 0.3 |
| ⁴ SO ₄ | mg. L ⁻¹ | 400 | ¹⁴ EC | μS/cm | 350 |
| ⁵ Na | mg. L ⁻¹ | 200 | ¹⁵ Hn | mg. L ⁻¹ CaCO ₃ | 500 |
| ⁶ Ca | mg. L ⁻¹ | 250 | ¹⁶ HCO ₃ | - | - |
| ⁷ Mg | mg. L ⁻¹ | 100 | ¹⁷ Si | - | - |
| ⁸ Cl | mg. L ⁻¹ | 2 | ¹⁸ Sr | - | - |
| ⁹ K | mg. L ⁻¹ | 10 | ¹⁹ Ba | mg. L ⁻¹ | 1 |
| ¹⁰ Mn | mg. L ⁻¹ | 0.1 | - | - | - |
| ¹ NO ₃ : Nitrate; ² DR: Evaporative resistance; ³ pH: Hydrogen potential; ⁴ SO ₄ : Sulfate; ⁵ Na: Sodium; ⁶ Ca: Calcium; ⁷ Mg: Magnesium; ⁸ Cl: Chlorine; ⁹ K: Potassium; ¹⁰ Mn: Manganese; ¹¹ F: Fluorine; ¹² Zn: Zinc; ¹³ Fe: Iron; ¹⁴ EC: Electrical conductivity; ¹⁵ Hn: Hardness; ¹⁶ HCO ₃ : Bicarbonate; ¹⁷ Si: Silicon; ¹⁸ Sr: Strontium; ¹⁹ Ba: Barium. | | | | | |

2.3. Piper's diagram

The Piper diagram was constructed and applied in the classification and comparison of distinct groups of water, associated with dominant cations and anions, also called tri-linear diagrams, in this type of representation, the concentrations of each ion analyzed were given in percentages, as well, plotting the proportions of the main cations (Ca⁺², Mg⁺², Na⁺ and K⁺) and the main anions (HCO⁻³, Cl⁻ and SO⁻⁴) in two respective triangular diagrams, combining the information from the two triangles in a rhombus located between them, with the main types of chemical constituents of water (Piper, 1944; Anders et al., 2014; Yang et al., 2016).

The proportions were plotted in triangular graphical representations and their scales, for the proportion of the variables, corresponding to 100%. The representations show the relative proportions of the main ions, but not their absolute concentrations. The procedure for plotting a point in Piper's diagram consisted of entering the percentage of certain cations and anions, in the triangular bases, and a line was drawn corresponding to the value of this percentage. The crossing of the lines drawn on the triangular bases for

the cations and anions determined the point that is transcribed in the central diamond, where the hydrochemical classification of the water is. The software used for processing Piper's diagram was Grapher version 13.

2.4. Hydrogeological and hydrochemical map

Based on the database provided by the Brazilian Institute of Geography and Statistics (IBGE), the hydrogeological (IBGE, 2018) and hydrochemical (IBGE, 2020) map of the study region was generated.

The hydrogeological map of NEB cartographically represents the productivity of aquifers in this region, based on the values of flows and specific flows of 54,864 tubular wells. Such information is stored in a database, with the procedures used in the Map of Hydrogeological Domains/Subdomains of Brazil and the Hydrogeological Charters of Brazil to the Millionth (CPRM, 2007).

The hydrochemical map of NEB's underground water sources brings together a collection of 10,478 hydrochemical analyzes, all from tubular wells and chemically homogeneous domains concerning potability, chemical facies, and the suitability of water for use in irrigation. The chemical reports were incorporated into a database (elaborated in Access), where they were classified in terms of potability, chemical facies, and the suitability of waters for use in irrigation, and represented in a shapefile format.

These determinations were migrated and georeferenced in GeoMedia, where work was carried out to individualize chemically homogeneous zones, using geological, physiographic, and hydrogeological criteria, which allowed the demarcation of units that have similar characteristics within their limits.

The data made available on the platform are in the shapefile format, with an established pre-classification, in which reclassification techniques by geoprocessing were applied to reclassify these shapefiles, for the area comprising the study. The shapefiles were processed using ArcGIS® software, version 10.2.2 (ESRI, Redlands, California, USA).

2.5. Statistical analysis

The data obtained were subjected to analysis of descriptive statistics based on the mean, median, and coefficient of variation (CV, %), being classified as low when the $CV < 12\%$; medium when $12\% < CV < 24\%$, and high when $CV > 24\%$ (Warrick and Nielsen, 1980). Subsequently, the Kolmogorov-Smirnov normality test (KS test) was applied with a significance level set at $p \leq 0.01$.

The geostatistics analysis was performed based on the calculation of the classic semivariances (Eq. 1), which estimated the structure and the spatial dependence between the pairs of observations.

$$\gamma(h) = \frac{1}{2N(h)} \sum_{i=1}^{N(h)} [Z(X_i) - Z(X_i + h)]^2 \quad (1)$$

where,

$\gamma(h)$ - is the experimental semi-variance estimator, obtained from the sampled values $Z(X_i)$, $Z(X_i+h)$;

$N(h)$ - is the number of measured value pairs separated by the vector or delay distance;

h - is the distance between sample pairs (i.e., it is the distance between two samples);

$Z(X_i)$ and $Z(X_i + h)$ - are the values of the i -th observation of the regionalized variable, collected at points X_i and X_i+h ($i = 1, \dots, n$), separated by the vector h .

Spatial dependence was analyzed by adjusting the semivariogram based on the estimate of the semivariance using the GEO-EAS® program (England et al., 1989). The data were adjusted to the spherical, exponential, and Gaussian models (Eqs. 2, 3, and 4), respectively, according to Deutsch et al. (1998). The spherical, exponential, and Gaussian models are referred to in the literature as transitive theoretical models and are more common for adjusting semivariograms (Gois et al., 2015).

Spherical Model:

$$\gamma(h) = \begin{cases} C_0 + C \cdot \left[1.5 \frac{h}{a} - 0.5 \left(\frac{h}{a} \right)^3 \right], & \text{for } 0 \leq h \leq a \\ C_0 + C, & \text{for } h > a \end{cases} \quad (2)$$

Exponential Model:

$$\gamma(h) = C_0 + C \cdot \left[1 - \exp\left(-\frac{3h}{a}\right) \right]$$

3

Gaussian model:

$$\gamma(h) = C_0 + C \cdot \left[1 - \exp\left(-\frac{(3h)^2}{a^2}\right) \right] \quad (4)$$

where,

$\gamma(h)$ - is the experimental semi-variance estimator;

C_0+C - is the sill (i.e., it is the nugget effect plus the variance dispersion, given by the acronyms C_0 and C , respectively);

h - is the distance between sample pairs;

a - is the range (m).

The best models of the adjusted semivariograms were validated by the cross-validation of the Jack-Knifing test, in which the mean must be close to zero and the standard deviation close to 1 (e.g., Vauclin et al., 1983), the program used for that analysis was GEO-EAS® (England et al., 1989).

The degree of spatial dependence (DSD) was classified according to Cambardella et al. (1994), which suggests strong dependence (St) (DSD < 25%); moderate dependence (Md) (DSD between 25 and 75%), and weak dependence (We): (DSD > 75%). For making the kriging maps, the Surfer 9 program (Golden Software, 2010) was used.

For principal component analysis (PCA), 19 variables were admitted. Based on the principal components (PC), the covariance matrix was obtained to extract the eigenvalues that originate the eigenvectors. To identify the variables that presented correlation, the Kaiser criterion was used, considering the eigenvalues greater than 1.0, which generate components with a relevant amount of information contained in the original data (Kaiser, 1958).

Pearson's correlation (r) was also performed for all variables, seeking to correlate with the PCA, to highlight the similarities between the variables. The program used for PCA and the correlation r was RStudio, version 3.6.1 (R Core Team, 2019).

Linear regression models were established to justify and clarify the main hydrochemical characteristics that are correlated with nitrate (NO_3), a component that has a direct impact on human health. It was verified among the main variables, the one with the highest coefficient of determination ($R^2 > 0.5$) to reduce the main relevance and correlation with NO_3 . The analyzes were performed using the Minitab software, version 19.

3. Results And Discussion

3.1. Hydrogeological and hydrochemical characterization of the Beberibe aquifer

Figure 3 shows spatially the hydrogeological characterization of the groundwater of the Beberibe aquifer. Most of the artesian wells in the mineral water production units are close to the coast, a densely populated region (Figures 1 and 3). The artesian wells close to the coast are of porous geological formation, with the lowest altitudes (Figure 2), with flow variations from medium to very high. From the western portion of the study region, there is a fissural geological formation, considering the higher altitudes, with greater rocky extension and flow variations from medium to very high (Figures 2 and 3).

[INSERT TO FIGURE 3 HERE]

There is a specific homogeneous flow occurring close to the coastal region, categorized as “very high productivity” (Figure 3). The obtained result corroborates with the studies carried out by Hu et al. (2017) who analyzed the hydrogeological configuration of groundwater for the entire Brazilian territory and

highlighted good water retention capacity for recharging and discharging aquifers. The authors also pointed out that the aquifers close to the Atlantic Ocean play a role as a “wall or barrier”, because the water tables in these regions always remain at the same level as the sea surface at the limits of the coast, thus maintaining better retention, which will lead to homogenization of water flow.

Although the original depth of the well is unknown, part of the water may come from shallower horizons (Pernambuco coast) and another part may come from the western region of the state, via deeper horizons, in superior topographic conditions. Such observations are in line with Silva et al. (2020), who studied the predominant hydrochemical mechanisms and processes that control the hydrochemistry of groundwater in a region of Acre, Northern Brazil, that regardless of the knowledge of the depth of the well, the origin of the water can come from different horizons, again highlighting the topographic conditions under the influence of a given region.

Figure 4 highlights the hydrochemical characterization of the groundwater in the Beberibe aquifer. It appears that in all of the sampled points (artesian wells), the waters are of the mixed bicarbonate type (Bm) and high potability for human consumption (IBGE, 2020). However, one should not only consider the hydrochemical reactions that occur in the Beberibe aquifer, but also the anthropic actions that occur in RMRE.

[INSERT TO FIGURE 4 HERE]

The composition of groundwater can provide relevant information about interactions in aquifers since hydrochemistry is the result of specific reactions related to rock-water interactions that vary within an aquifer unit (Teramoto et al., 2020). Consequently, the interpretation of aquifer mineralogy and water chemistry data may indicate the transport of groundwater within and between aquifers.

As recently highlighted by Teramoto et al. (2020), the hydrochemistry in the Guarani aquifer, due to its mixed bicarbonate composition, influences the geological formation of the porous type. This statement is confirmed in the present study since the geological composition is heterogeneous and presents an advanced state of decomposition, which implies a high variability of bicarbonates.

3.2. Piper's diagram

The hydrochemical face is a term used to describe the percentage of the chemical composition of the water, resulting from the combined effect of the solution's kinetics, rock-water interactions, hydrogeological configurations, and sources of contamination. Piper's trilinear diagram (Piper, 1944) consists of a diamond and a pair of equilateral triangles, in which two triangles represent the anion and the cation, respectively, connected by a diamond-shaped diagram. Figure 5 shows the hydrochemical composition of the groundwater in the Beberibe aquifer.

[INSERT TO FIGURE 5 HERE]

The chemical composition of groundwater is mainly of the Na-K-Cl-SO₄ type (Figure 5), where Na-K corresponds to approximately 90% in the first triangle. The hydrochemical type Ca-Mg-Cl-SO₄ also appeared in Piper's diagram, to which, Ca-Mg corresponded to 20% of the composition. Na⁺ is the dominant cation and Cl⁻ is the dominant anion, while Ca²⁺, Mg²⁺, and HCO³⁻ are not predominant. The chemical facies Na-Cl indicate a low flow in the aquifer that allows the predominance of Na⁺ as a result of the ion exchange process against Ca²⁺. There was a high concentration of Cl⁻ in all samples, which suggests an evaporation process in the Beberibe aquifer.

Sargazi et al. (2020), evaluated the quality of groundwater in the city of Zahedan, Sistan, and the province of Baluchestan, in Iran, and the results of the hydrochemical composition of the waters via the Piper diagram, are similar to the results obtained in the study, where the authors pointed out the predominance of Na-Cl-SO₄ and Ca-Mg-Cl-SO₄, in the studied waters. Like Iqbal et al. (2018) and Pazand et al. (2018) studied the hydrochemical composition of groundwater in Abu Dhabi - United Arab Emirates and in the Ardestan basin in Central Iran, respectively, showed results similar to the study.

3.3. Descriptive statistics and geostatistics of the data

Table 2 shows the temporal variability based on descriptive statistics (see section 2.5), for the hydrochemical parameters of the mineral water in the Beberibe aquifer. According to the criteria of Warrick and Nielsen (1980), the CV% presented values of medium too high for all the studied variables, in which the average variation (14.77%) was only for the hydrogen potential (pH), for the other variables had a high variation, CV > 29%. All parameters showed normal distribution, according to the KS test at the level of 1% probability.

Table 2
Descriptive statistics of the hydrochemical parameters of mineral water.

| Variable | Mean | Median | ²⁰ Min | ²¹ Max | ²² CV | ²³ SD | ²⁴ A | ²⁵ K |
|---|-------|--------|-------------------|-------------------|------------------|------------------|-----------------|-----------------|
| ¹ NO ₃ | 4.53 | 1.29 | 0.15 | 43.25 | 195.14 | 8.83 | 3.52 | 12.91 |
| ² DR | 66.17 | 57.90 | 20.00 | 124.98 | 42.13 | 27.87 | 0.61 | -0.42 |
| ³ pH | 5.31 | 5.41 | 4.10 | 7.70 | 14.77 | 0.78 | 1.32 | 2.77 |
| ⁴ SO ₄ | 3.77 | 2.03 | 0.00 | 18.25 | 105.64 | 3.98 | 2.54 | 6.32 |
| ⁵ Na | 9.21 | 8.69 | 5.00 | 19.94 | 29.44 | 2.71 | 2.04 | 6.59 |
| ⁶ Ca | 0.90 | 0.61 | 0.00 | 2.66 | 77.37 | 0.70 | 0.96 | 0.12 |
| ⁷ Mg | 1.44 | 1.00 | 0.40 | 5.30 | 77.84 | 1.12 | 2.04 | 4.03 |
| ⁸ Cl | 12.27 | 11.97 | 0.12 | 26.51 | 40.00 | 4.91 | 0.29 | 3.34 |
| ⁹ K | 4.29 | 4.65 | 0.00 | 10.45 | 81.45 | 3.50 | 0.17 | -1.47 |
| ¹⁰ Mn | 0.03 | 0.00 | 0.00 | 0.85 | 485.27 | 0.15 | 5.75 | 33.30 |
| ¹¹ F | 0.04 | 0.00 | 0.00 | 0.85 | 361.79 | 0.15 | 5.51 | 31.31 |
| ¹² Zn | 0.01 | 0.01 | 0.00 | 0.08 | 166.80 | 0.02 | 2.51 | 6.71 |
| ¹³ Fe | 0.06 | 0.02 | 0.00 | 0.38 | 186.85 | 0.11 | 2.27 | 3.93 |
| ¹⁴ EC | 86.88 | 78.70 | 40.00 | 197.00 | 41.64 | 36.18 | 1.68 | 3.14 |
| ¹⁵ Hn | 9.68 | 7.13 | 4.86 | 30.50 | 62.85 | 6.08 | 1.82 | 3.36 |
| ¹⁶ HCO ₃ | 8.94 | 8.48 | 0.00 | 22.87 | 71.13 | 6.36 | 0.40 | -0.70 |
| ¹⁷ Si | 13.43 | 13.99 | 0.00 | 43.66 | 66.33 | 8.91 | 0.89 | 2.71 |
| ¹⁸ Sr | 0.01 | 0.01 | 0.00 | 0.05 | 143.13 | 0.01 | 1.85 | 3.28 |
| ¹⁹ Ba | 0.04 | 0.01 | 0.00 | 0.23 | 138.00 | 0.06 | 1.62 | 2.78 |
| ¹ NO ₃ : Nitrate; ² DR: Evaporative resistance; ³ pH: Hydrogen potential; ⁴ SO ₄ : Sulfate; ⁵ Na: Sodium; ⁶ Ca: Calcium; ⁷ Mg: Magnesium; ⁸ Cl: Chlorine; ⁹ K: Potassium; ¹⁰ Mn: Manganese; ¹¹ F: Fluorine; ¹² Zn: Zinc; ¹³ Fe: Iron; ¹⁴ EC: Electrical conductivity; ¹⁵ Hn: Hardness; ¹⁶ HCO ₃ : Bicarbonate; ¹⁷ Si: Silicon; ¹⁸ Sr: Strontium; ¹⁹ Ba: Barium; ²⁰ Min: Minimum; ²¹ Max: Maximo; ²² CV: Coefficient of variation; ²³ SD: Standard deviation; ²⁴ A: Asymmetry; and ²⁵ K: Kurtosis. | | | | | | | | |

The variability between the medium and high categories is mainly due to the hydrogeological and hydrochemical diversity, which in turn occurs in the geological formation of rocks and which has a direct impact on the chemistry of groundwater (IBGE, 2018; IBGE, 2020). The results obtained corroborate those mentioned by Yang et al. (2020), where they investigated the hydrochemical composition of groundwater to highlight its quality and assess its risk/suitability for irrigation purposes in the Ordos Basin, China, they identified high CV% for all variables studied, except for the pH, where the CV% presented a value referring to the medium variability.

The highest CV% indicated that the ions were sensitive to the external environment, such as hydrological conditions, topography, and anthropogenic activities, as discussed by Yang et al. (2020). Another key factor is pH, which according to Liu et al. (2018), in a study of the dynamic characteristics of groundwater in the valley plain of the city of Lhasa (capital of the Autonomous Region of Tibet), the low CV% indicated that the pH of groundwater tends to be relatively stable, which differs from the present study, in which the pH was not stable and CV% is admitted with medium variability, according to the criterion of Warrick and Nielsen (1980) - (Table 2).

The pH according to the standards established in Table 1 and compliance with the minimum values recorded in Table 2, presented low standards, indicative of points of distribution of acidic mineral water for human health. High concentrations of NO_3 were observed in some mineral water distribution points, therefore, outside the limits established by Brazilian legislation (Table 1), probably caused by the socio-economic development of the study region, as highlighted earlier by Liu et al. (2018).

The electrical conductivity (EC) showed high CV%, due to the oscillation of salinity in urban areas (natural effect due to the rock/soil factor, and anthropization), such variations are characteristics of low permeability and low hydraulic gradient, due to the dilution effect salts during the rainy season and evaporation in the dry season. The results similar to those obtained by Tlili-Zrelli et al. (2015), they studied the hydrogeochemistry of groundwater in an alluvial aquifer in northern Tunisia, where the zones of low permeability and low hydraulic gradient, occur due to the dilution effect of salts during the rainy season and evaporation during the dry season, which favors a high variability in the levels of salts diluted in the water due to the climate and the greater and/or less water availability.

The analysis of the spatial variability for the hydrochemical parameters is shown in Table 3. All the parameters evaluated, the Gaussian model was the one that best fit, which is indicated for studies of groundwater. The highlight for the coefficient R^2 with variations between 0.6 to 0.99.

Table 3

Analysis of spatial variability followed by adjusted semivariograms for the hydrochemical parameters of mineral water.

| ²⁰ Var | ²¹ Mo | ²² C ₀ | ²³ C ₀ +C | ²⁴ a | ²⁵ R ² | ²⁶ C ₀ | ²⁷ DSD | Jack-Knifing | |
|--------------------------------|------------------|------------------------------|---------------------------------|-----------------|------------------------------|------------------------------|-------------------|-----------------|------------------|
| | | | | | | (C ₀ +C) | | ²⁸ m | ²⁹ SD |
| ¹ NO ₃ | Gau | 2.000 | 10.500 | 25000.000 | 0.800 | 19.047 | Ft | -0.082 | 1.017 |
| ² DR | Gau | 90.000 | 1396.000 | 4886.115 | 0.849 | 6.446 | Ft | 0.006 | 1.007 |
| ³ pH | Gau | 0.128 | 1.975 | 14440.107 | 0.933 | 6.481 | Ft | 0.070 | 0.998 |
| ⁴ SO ₄ | Gau | 0.200 | 3.000 | 100.000 | 0.599 | 6.667 | Ft | -0.087 | 1.113 |
| ⁵ Na | Gau | 3.000 | 18.900 | 20000.000 | 0.728 | 15.873 | Ft | 0.012 | 1.044 |
| ⁶ Ca | Gau | 0.120 | 0.491 | 417.424 | 0.713 | 24.439 | Ft | -0.048 | 1.041 |
| ⁷ Mg | Gau | 0.136 | 1.292 | 3360.178 | 0.908 | 10.526 | Ft | -0.011 | 0.940 |
| ⁸ Cl | Gau | 5.000 | 28.000 | 13000.000 | 0.701 | 17.857 | Ft | 0.050 | 1.049 |
| ⁹ K | Gau | 4.000 | 22.000 | 5000.000 | 0.708 | 18.182 | Ft | 0.029 | 1.061 |
| ¹⁰ Mn | Gau | 1.50E-05 | 1.54E-04 | 16956.777 | 0.657 | 9.740 | Ft | 0.027 | 1.081 |
| ¹¹ F | Gau | 1.00E-06 | 1.00E-02 | 1000.000 | 0.989 | 0.010 | Ft | -0.056 | 1.112 |
| ¹² Zn | Gau | 2.00E-04 | 0.724 | 8861.172 | 0.935 | 0.027 | Ft | 0.049 | 1.032 |
| ¹³ Fe | Gau | 1.00E-6 | 0.002 | 169.741 | 0.917 | 4.234E-4 | Ft | 0.017 | 1.028 |
| ¹⁴ EC | Gau | 80.000 | 557.100 | 2468.172 | 0.961 | 14.360 | Ft | -0.057 | 1.070 |
| ¹⁵ Hn | Gau | 12.000 | 60.000 | 12500.000 | 0.790 | 20.000 | Ft | 0.017 | 1.071 |
| ¹⁶ HCO ₃ | Gau | 25.000 | 110.000 | 4200.000 | 0.812 | 22.727 | Ft | 0.023 | 1.053 |

¹NO₃: Nitrate; ²DR: Evaporative resistance; ³pH: Hydrogen potential; ⁴SO₄: Sulfate; ⁵Na: Sodium; ⁶Ca: Calcium; ⁷Mg: Magnesium; ⁸Cl: Chlorine; ⁹K: Potassium; ¹⁰Mn: Manganese; ¹¹F: Fluorine; ¹²Zn: Zinc; ¹³Fe: Iron; ¹⁴EC: Electrical conductivity; ¹⁵Hn: Hardness; ¹⁶HCO₃: Bicarbonate; ¹⁷Si: Silicon; ¹⁸Sr: Strontium; ¹⁹Ba: Barium; ²⁰Var: Variable; ²¹Mo: Model; ²²C₀: Nugget effect; ²³C₀+C: Sill; ²⁴a: Range; ²⁵R²: Coefficient of determination; ²⁶C₀/(C₀+C): Degree of spatial dependence (%); ²⁷DSD: Class of the degree of spatial dependence; ²⁸m: Mean; ²⁹SD: Standard deviation; Gau: Gaussian; Ft: Strong.

| ²⁰ Var | ²¹ Mo | ²² C ₀ | ²³ C ₀ +C | ²⁴ a | ²⁵ R ² | ²⁶ C ₀ | ²⁷ DSD | Jack-Knifing | |
|-------------------|------------------|------------------------------|---------------------------------|-----------------|------------------------------|------------------------------|-------------------|-----------------|------------------|
| | | | | | | (C ₀ +C) | | ²⁸ m | ²⁹ SD |
| ¹⁷ Si | Gau | 50.000 | 210.000 | 7000.000 | 0.905 | 23.810 | Ft | 0.049 | 1.004 |
| ¹⁸ Sr | Gau | 5.00E-06 | 7.30E-05 | 803.671 | 0.867 | 6.849 | Ft | -0.053 | 1.246 |
| ¹⁹ Ba | Gau | 8.00E-04 | 0.021 | 4588.202 | 0.630 | 3.810 | Ft | -0.010 | 1.080 |

¹NO₃: Nitrate; ²DR: Evaporative resistance; ³pH: Hydrogen potential; ⁴SO₄: Sulfate; ⁵Na: Sodium; ⁶Ca: Calcium; ⁷Mg: Magnesium; ⁸Cl: Chlorine; ⁹K: Potassium; ¹⁰Mn: Manganese; ¹¹F: Fluorine; ¹²Zn: Zinc; ¹³Fe: Iron; ¹⁴EC: Electrical conductivity; ¹⁵Hn: Hardness; ¹⁶HCO₃: Bicarbonate; ¹⁷Si: Silicon; ¹⁸Sr: Strontium; ¹⁹Ba: Barium; ²⁰Var: Variable; ²¹Mo: Model; ²²C₀: Nugget effect; ²³C₀+C: Sill; ²⁴a: Range; ²⁵R²: Coefficient of determination; ²⁶C₀/(C₀+C): Degree of spatial dependence (%); ²⁷DSD: Class of the degree of spatial dependence; ²⁸m: Mean; ²⁹SD: Standard deviation; Gau: Gaussian; Ft: Strong.

Yin et al. (2019), analyzed geostatistically the hydrochemical variations and the causes of NO₃ pollution of groundwater in a plain in southern Beijing, China. They highlighted the need for interactions between the transitive theoretical models to validate the best for each parameter. However, in the present study, cross-validation by Jack-Knifing (Vauclin et al., 1983) was applied, were all established semivariograms presented the mean close to 0 and the standard deviation close to 1, and thus used in kriging maps for each studied hydrochemical variable (Table 3).

The DSD was strong for all the parameters analyzed, which indicates that the value of each parameter associated with a given location, was more similar to the value of a neighboring sample than to the rest of the location of the sample set, which reinforces the validation of the Gaussian model for the studied hydrochemical variables (Cambardella et al., 1994).

Figure 6 illustrates the spatial distribution of the hydrochemical parameters of the mineral water sources in the Beberibe aquifer in the study area. Based on the semivariograms, kriging of the maps was performed, according to each model generated for the hydrochemical variables of the groundwater, implementing the nugget effect, level, and range of each model.

[INSERT TO FIGURE 6 HERE]

NO₃ concentrations occurred mainly on the coast of Pernambuco, with an emphasis on the municipalities of Recife and Olinda (Figure 6). In both municipalities, the NO₃ concentrations were higher, mainly because these municipalities have a high population density and have a high flow of tourists, vegetable cultivation near rivers (causing eutrophication), as well as the holding of major cultural events, such as Carnival in the city of Recife and Olinda, Brazil, considered cities that host the carnival festival with the largest flow of people in the world, with an average of 1 million people a day. Within this theme, one of the

factors that imply high concentrations of NO_3 is caused by the high pollution generated by tourists and the consequent contamination of the main rivers, highlighting Capibaribe, Beberibe, and Tejipió.

Also noteworthy is the fact that the city of Recife is among the 10 largest Brazilian metropolises, with a population of 1.555 million inhabitants, according to the IBGE - (IBGE, 2020). In this context, the rate of pollution generated in the urban centers of the metropolis, associated with the lack of sanitation in neighborhoods, provides for the contamination of rivers, which in turn contribute to recharge the aquifer, which implies the contamination of groundwater and the increase of NO_3 concentration. Therefore, there is still the spread of waterborne diseases, mainly diarrhea, typhoid fever, hepatitis A, leptospirosis, cholera, and intestinal infections, caused by bacteria.

Concomitant with NO_3 concentrations, it is observed in the maps of the hydrochemical variables that the evaporative resistance (DR), sodium (Na), calcium (Ca), magnesium (Mg), chlorine (Cl), electrical conductivity (EC), hardness (Hn) and strontium (Sr), presented higher concentrations in the places with the highest concentration of NO_3 (Figure 6). From the coast that comprises the municipality of Recife and Olinda, it is where the greatest concentrations of these elements are found, among them are heavy metals and EC, which is associated with greater concentrations of soluble solids in water, which in turn correlate with anthropic pollution.

Corroborating the findings of the present study, Bodrud-Doza et al. (2016), carried out the characterization of groundwater quality based on water assessment indices, multivariate statistics, and geostatistics in central Bangladesh, and concluded that anthropogenic factors (e.g., industrial pollution, inadequate garbage discharge, inadequate sanitation) contribute groundwater quality. Bhuiyan et al. (2016) also assessed the groundwater quality of the Lakhimpur district in Bangladesh based on water quality indices, geostatistical methods, and multivariate analysis pointed out that a kriging method is an effective tool for decision-makers on groundwater quality management.

It is noteworthy that the hydrogeological formation also contributes to NO_3 concentrations. It appears that the Pernambuco coast has a hydrogeological formation of the mixed bicarbonate type (Figure 4), which because of this, there is a high variability ($> \text{CV}\%$) of the hydrochemical elements of groundwater (Table 2). This mixed diversity of bicarbonate can also be considered as one of the factors for this high concentration of NO_3 , as such regions are common of fissural geological formation, which in turn reflects and a greater tendency for contamination of these waters.

According to the Ministério da Saúde (1999), Ministério da Saúde (2006), and CETESB (2016), concentrations of NO_3 , DR, Na, Ca, Mg, Cl, EC, Hn and Sr, only NO_3 and Cl did not comply with Brazilian legislation, with values higher than allowed (Table 1). However, to the west of the coast, values were observed within the limits allowed for NO_3 and Cl, which reinforces the anthropogenic impact in the coastal region (Figure 6). Corroborating the findings of Yin et al. (2019), who claim that industrial areas and intense urbanization promote greater groundwater pollution by NO_3 .

The pH of groundwater on the coast met the acceptable standard for human health (pH between 6 and 9), with variations between acid to alkaline (pH between 6.4 and 7.6) (Ministério da Saúde, 1999; Ministério da Saúde, 2006; CETESB, 2016). However, the west region of the coast had a pH < 6 (Figure 6). Abu-alnaeem et al. (2018), evaluated the salinity and quality of groundwater in the Gaza coastal aquifer, Gaza Strip in Palestine, and highlighted that acidity and alkalinity close to neutralization, is derived from the dissolution of carbonate minerals in the form of bicarbonate (HCO_3^-). Corroborating the statement of the aforementioned authors, the coastal region of the present study, to the east, showed pH with variations between acid and alkaline, still because it presents mixed bicarbonate hydrogeological formation (Figure 4).

The elements SO_4 , K, Mn, F, Zn, Fe, HCO_3 , Si, Sr and Ba were the elements that had the highest concentrations west of the coast (Figure 6). This study region was also the one with the lowest pH. It is noteworthy that only the elements SO_4 , F, Zn, and Ba, presented concentrations within the quality standards for human consumption (Ministério da Saúde, 1999; Ministério da Saúde, 2006; CETESB, 2016). The elements K, Mn, and Fe showed values above that allowed by current legislation. HCO_3 , Si, and Sr, on the other hand, do not have a defined quality standard.

Hossain and Patra, (2020) carried out a contamination zoning and health risk assessment of trace elements in groundwater utilizing geostatistical modeling and reported that pH controls chemistry, which is a component that influences the hydrochemical standards of water and, thus, corroborates with the observations of the present study, in which the elements K, Mn, and Fe presented higher values for the region of lower pH.

3.4. Principal component analysis (PCA)

The PCA presents the eigenvalue, the proportion, and the accumulation of the total variance for all variables studied (Table 4). The cumulative total variance for principal component 2 (PC2) was 49.61%, a significant result for the analyzed data set. According to the criteria established by Kaiser (1958), PC1 and PC2 presented their eigenvalues greater than 1, which indicated a significant information load and, thus, generate the biplot graphs.

Table 4
Principal components of the hydrochemical parameters of mineral water.

| Components | Eigenvalue | Proportion (%) | Cumulative (%) |
|--------------------------|------------|----------------|----------------|
| PC1 | 6.30 | 33.14 | 33.14 |
| PC2 | 3.13 | 16.46 | 49.61 |
| PC: Principal component. | | | |

Yang et al. (2016) carried out the identification of hydrogeochemical processes and assessment of groundwater quality in the southeastern part of the Ordos basin in China, based on the PCA and obtained total cumulative variance for the PC2, of 59.26%, which is higher than the study.

In Figure 7, the PC's biplot chart stands out and Pearson correlation of the hydrochemical parameters of the mineral water of the Beberibe aquifer in the study area, referring to the municipalities of Recife, Olinda, Paulista, Camaragibe, São Lourenço da Mata, and Paudalho.

[INSERT TO FIGURE 7 HERE]

For the PC's, the 19 studied variables (NO_3 ; DR; pH; SO_4 ; Na; Ca; Mg; Cl; K; Mn; F; Zn; Fe; EC; Hn; HCO_3 ; Si; Sr and Ba) were admitted and the correlated points refer to the artesian sample collection wells (A01 to A34). The variables DR, Na, Ca, Mg, Cl, EC, Hn, and Sr, showed a correlation with NO_3 , as observed in kriging maps (Figure 7A). However, it is noteworthy that among the observed correlations, Cl was the one with the highest correlation with NO_3 , in which, the Cl projection line follows the NO_3 line, which characterizes this strong correlation (Figure 7B).

Similar results were found by Cao et al. (2020), where they studied the heterogeneity of an aquifer in a region of France, through PCA and observed a high correlation between Cl and NO_3 . The same results were found by Ayed et al. (2017), where they performed a hydrochemical characterization of groundwater using PCA for the southeastern region of Tunisia, and observed the same correlation between Cl and NO_3 .

To clarify more precisely the correlations between the variables, Pearson's correlation was applied, where the correlation was significant between Cl and NO_3 (Figure 7B). Corroborating the findings of this study, Ayed et al. (2017) also observed a strong correlation between Cl and NO_3 .

3.5. Linear regression analysis

Based on the analysis of the kriging maps (Figure 6) and the PCA - (Figure 7A), was performed a simple linear regression analysis of the electrical conductivity (EC), hardness (Hn), evaporative resistance (DR), magnesium (Mg), sodium (Na) and chlorine (Cl), with nitrate (NO_3), as they present a greater correlation with NO_3 in the previous analyzes (Figure 8). The R^2 criterion greater than 0.5 was established to represent only the most representative predictor variables with NO_3 .

[INSERT TO FIGURE 8 HERE]

Among the linear regressions, only $\text{NO}_3 \times \text{DR}$ showed $R^2 < 0.5$ ($R^2 = 0.32$), so the DR has no direct influence on NO_3 (Figure 8C). It can be seen that Cl, showed a satisfactory R^2 with NO_3 ($R^2 = 0.51$) - (Figure 8F), previously indicated by geostatistics based on kriging maps and PCA, and these two variables showed a high correlation between themselves. The results obtained corroborate those described by Tiwari et al. (2017), where they assessed the spatial distribution of groundwater quality and assessed regional suitability for drinking water in the Alwar region in India and found a strong correlation between NO_3 and Cl.

The variables EC ($R^2 = 0.68$), Hn ($R^2 = 0.57$), Mg ($R^2 = 0.67$) and Na ($R^2 = 0.56$), showed satisfactory R^2 , respectively. Such variables have a direct correlation with NO_3 , thus being potential variables in the

hydrochemical characterization of groundwater.

4. Conclusions

Based on Brazilian legislation, there are strategic wells that have a direct impact on human health and, therefore, there is a need to reanalyze possible approaches for improvements that support health and quality of life. The composition and hydrochemical quality of groundwater in the metropolitan region of Recife and the coast of Pernambuco are directly influenced by hydrogeology, topographic conditions, and urban infrastructure (urban density).

In geostatistical modeling, based on the Gaussian model, it stands out concerning the other transitive theoretical models in the hydrochemical characterization of the waters of the Beberibe aquifer and thus spatially displays the spatial dynamics of water composition and quality in the study area with greater accuracy. Multivariate analysis via PCA associated with Pearson's correlation is a promising technique for assessing the hydrochemistry of groundwater in the Beberibe aquifer together with the hydrogeological and hydrochemical maps of groundwater made it possible to efficiently characterize water quality standards for the coast of Pernambuco.

The anthropogenic influence of the metropolitan center of Recife, has a direct impact on water quality for human health, especially on nitrate concentrations (NO_3). It is also noteworthy that the concentrations of chlorine (Cl) have a high correlation with NO_3 , being confirmed in the kriging maps and the PCA, Pearson's correlation, and in the linear regression. Other methodologies must be formulated and applied, to confirm or rule out the possibility of recharging the regional flow of groundwater. The methodology adopted in the study can be perfectly applied in other regions of the planet with conditions of social vulnerability and problems with water quality, with bias of monitoring and definition of public policies.

Low-quality underground water should not be used for human consumption, as it becomes the main agent for the emergence of waterborne diseases, mainly diarrhea, typhoid fever, hepatitis A, leptospirosis, cholera, and intestinal infections, caused by bacteria, which it reaches from infants to the elderly, especially those who live in areas of social vulnerability and with low-quality water. Therefore, regular monitoring is essential to ensure good quality water and a healthy environment that provides quality of life for local families.

Declarations

5. Acknowledgment

To the *Programa de Pós-Graduação em Engenharia Agrícola* (PGEA), *Programa de Pós-graduação em Química* (PPGQ), and the *Grupo de Pesquisa em Ambiente* (GPESA) of the Federal Rural University of Pernambuco (UFRPE) for supporting the development of this research. The *Coordenação de Aperfeiçoamento de Pessoal de Nível Superior* (CAPES - Finance Code 001) and the *Fundação de Amparo à Ciência e Tecnologia do Estado de Pernambuco* (FACEPE), for the financing of scholarships. The third

and fourth authors are grateful for the Research Productivity grant from the *Conselho Nacional de Desenvolvimento Científico e Tecnológico* (CNPq) level 2 under process number 304060/2016-0 and 309681/2019-7, respectively.

References

1. ABINAM (2020) *Associação Brasileira Indústria Águas Minerais*. [online]. Available at:. [Accessed 15 July 2020]
2. Abu-alnaeem MF, Yusoff I, Ng TF, Alias Y, Raksmeiy M (2018) Assessment of groundwater salinity and quality in Gaza coastal aquifer, Gaza Strip, Palestine: An integrated statistical, geostatistical and hydrogeochemical approaches study. *Sci Total Environ* 615:972–989. <https://doi.org/10.1016/j.scitotenv.2017.09.320>
3. Agência Pernambucana de Vigilância Sanitária – APEVISA (2020) Programa de Monitoramento e Fiscalização da Água Envasada (Pura). [online]. Available at:. [Accessed 11 January 2021]
4. Anders R, Mendez GO, Futa K, Danskin WR (2014) A geochemical approach to determine sources and movement of saline groundwater in a coastal aquifer. *Groundwater* 52(5):756–768. <https://doi.org/10.1111/gwat.12108>
5. Arshad S, Mobeen M, Bashir S, Aziz T, Rehman A (2019) Spatializing Groundwater Quality Parameters and Their Impacts on Land Value in Khushab City, Punjab, Pakistan. *International Journal of Economic and Environmental Geology* 10(3):78–84. <https://doi.org/10.46660/ijeeg.vol11.iss1.1919>
6. Ayed B, Jmal I, Sahal S, Mokadem N, Saidi S, Boughariou E, Bouri S (2017) Hydrochemical characterization of groundwater using multivariate statistical analysis: the Maritime Djeffara shallow aquifer (Southeastern Tunisia). *Environ Earth Sci* 76(24):821. <https://doi.org/10.1007/s12665-017-7168-6>
7. Beck HE, Zimmermann NE, McVicar TR, Vergopolan N, Berg A, Wood EF (2018) Present and future Köppen-Geiger climate classification maps at 1-km resolution. *Scientific Data* 5:180214. <https://doi.org/10.1038/sdata.2018.214>
8. Bhuiyan MAH, Bodrud-Doza M, Islam AT, Rakib MA, Rahman MS, Ramanathan AL (2016) Assessment of groundwater quality of Lakshimpur district of Bangladesh using water quality indices, geostatistical methods, and multivariate analysis. *Environ Earth Sci* 75(12):1020. <https://doi.org/10.1007/s12665-016-5823-y>
9. Bodrud-Doza M, Bhuiyan MAH, Islam SDU, Rahman MS, Haque MM, Fatema KJ, Rahman MA (2019) Hydrogeochemical investigation of groundwater in Dhaka City of Bangladesh using GIS and multivariate statistical techniques. *Groundwater for Sustainable Development* 8:226–244. <https://doi.org/10.1016/j.gsd.2018.11.008>
10. Bodrud-Doza M, Islam AT, Ahmed F, Das S, Saha N, Rahman MS (2016) Characterization of groundwater quality using water evaluation indices, multivariate statistics and geostatistics in central Bangladesh. *Water Science* 30(1):19–40. <https://doi.org/10.1016/j.wsj.2016.05.001>

11. Bulia IL, Enzweiler J (2018) The hydrogeochemistry of bottled mineral water in São Paulo state, Brazil. *J Geochem Explor* 188:43–54. <https://doi.org/10.1016/j.gexplo.2018.01.007>
12. Cambardella CA, Moorman TB, Novak JM, Parkin TB, Karlen DL, Turco RF, Konopka AE (1994) Field-scale variability of soil properties in central Iowa soils. *Soil Science Society Amsterdam Journal* 58:1501–1511. <https://doi.org/10.2136/sssaj1994.03615995005800050033x>
13. Cao F, Jaunat J, Vergnaud-Ayraud V, Devau N, Labasque T, Guillou A, Ollivier P (2020) Heterogeneous behaviour of unconfined Chalk aquifers infer from combination of groundwater residence time, hydrochemistry and hydrodynamic tools. *J Hydrol* 581:124433. <https://doi.org/10.1016/j.jhydrol.2019.124433>
14. CETESB. (2016). *QUALIDADE DAS ÁGUAS SUBTERRÂNEAS NO ESTADO DE SÃO PAULO*. [online]. Available at: <https://cetesb.sp.gov.br/aguas-subterraneas/wp-content/uploads/sites/13/2013/11/Cetesb_QualidadeAguasSubterraneas2015_Web_20-07.pdf>. [Accessed 29 July 2020].
15. CPRH. (2020). *RECURSOS HÍDRICOS SUBTERRÂNEOS*. [online]. Available at: <http://www.cprh.pe.gov.br/downloads/25_Recurso_Hidricos_Subterraneos.pdf>. [Accessed 22 July 2020].
16. CPRM. (2007). *Mapa de Domínios/Subdomínios Hidrogeológicos do Brasil 1:2.500.000*. [online]. Available at: <<http://www.cprm.gov.br/publique/Hidrologia/Mapas-e-Publicacoes/Mapa-de-Dominios%7CSubdominios-Hidrogeologicos-do-Brasil-1%3A2.500.000-632.html>>. [Accessed 1 July 2020].
17. Deutsch CV, Journel AG (1998) *GSLIB Geostatistical Software Library and User's Guide*, Second edn. Oxford University Press, New York, p 369
18. England EJ, Sparks A, Robinson MD (1989) Geo—EAS (Geostatistical Environmental Assessment Software). *Environmental Software* 4(2):70–75. [https://doi.org/10.1016/0266-9838\(89\)90033-6](https://doi.org/10.1016/0266-9838(89)90033-6)
19. Gilabert-Alarcón C, Daesslé LW, Salgado-Méndez SO, Pérez-Flores MA, Knöller K, Kretschmar TG, Stumpp C (2018) Effects of reclaimed water discharge in the Maneadero coastal aquifer, Baja California, Mexico. *Appl Geochem* 92:121–139. <https://doi.org/10.1016/j.apgeochem.2018.03.006>
20. Gois G, Delgado RC, de Oliveira Júnior JF (2015) Modelos teóricos transitivos aplicados na interpolação espacial do Standardized Precipitation Index (SPI) para os episódios de El Niño forte no Estado do Tocantins, Brasil. *Irriga* 20(2):371–387. <https://doi.org/10.15809/irriga.2015v20n2p371>
21. GOLDEN SOFTWARE (2010) *Surfer for windows version 9.0*. Golden, Colorado, p 66
22. Gu X, Xiao Y, Yin S, Pan X, Niu Y, Shao J, Hao Q (2017) Natural and anthropogenic factors affecting the shallow groundwater quality in a typical irrigation area with reclaimed water, North China Plain. *Environ Monit Assess* 189(10):514. <https://doi.org/10.1007/s10661-017-6229-3>
23. Guadayol M, Cortina M, Guadayol JM, Caixach J (2016) Determination of dimethyl selenide and dimethyl sulphide compounds causing off-flavours in bottled mineral waters. *Water Res* 92:149–155. <https://doi.org/10.1016/j.watres.2016.01.016>

24. Hossain M, Patra PK (2020) Contamination zoning and health risk assessment of trace elements in groundwater through geostatistical modelling. *Ecotoxicol Environ Saf* 189:110038. <https://doi.org/10.1016/j.ecoenv.2019.110038>
25. Hu K, Awange JL, Forootan E, Goncalves RM, Fleming K (2017) Hydrogeological characterisation of groundwater over Brazil using remotely sensed and model products. *Sci Total Environ* 599:372–386. <https://doi.org/10.1016/j.scitotenv.2017.04.188>
26. Huang L, Liu Y (2017) Health information and consumer learning in the bottled water market. *Int J Ind Organ* 55:1–24. <https://doi.org/10.1016/j.ijindorg.2017.08.002>
27. IBGE (2018) Levantamento hidrogeológico. [online]. Available at: vN7H6tMg3R_3AI01ndqVTgh3mr000>. [Accessed 5 July 2020].
28. IBGE (2020) Hidroquímica subterrânea. [online]. Available at: . [Accessed 5 July 2020]
29. Iqbal J, Nazzal Y, Howari F, Xavier C, Yousef A (2018) Hydrochemical processes determining the groundwater quality for irrigation use in an arid environment: The case of Liwa Aquifer, Abu Dhabi, United Arab Emirates. *Groundwater for Sustainable Development* 7:212–219. <https://doi.org/10.1016/j.gsd.2018.06.004>
30. Jang CS (2015) Geostatistical analysis for spatially characterizing hydrochemical features of springs in Taiwan. *Environ Earth Sci* 73(11):7517–7531. <https://doi.org/10.1007/s12665-014-3924-z>
31. Kaiser HF (1958) The varimax criterion for analytic rotation in factor analysis. *Psychometrika* 23(3):187–200. <https://doi.org/10.1007/BF02289233>
32. Kunrath CCN, Patrocínio DC, Rodrigues MAS, Benvenuti T, Amado FDR (2020) Electrodialysis reversal as an alternative treatment for producing drinking water from brackish river water: A case study in the dry season, northeastern Brazil. *Journal of Environmental Chemical Engineering* 8(2):103719. <https://doi.org/10.1016/j.jece.2020.103719>
33. Liu J, Gao Z, Wang M, Li Y, Ma Y, Shi M, Zhang H (2018) Study on the dynamic characteristics of groundwater in the valley plain of Lhasa City. *Environ Earth Sci* 77(18):646. <https://doi.org/10.1007/s12665-018-7833-4>
34. Ministério da Saúde. (1999). *PORTARIA Nº 26, DE 15 DE JANEIRO DE 1999*. [online]. Available at: http://bvsms.saude.gov.br/bvs/saudelegis/anvisa/1999/prt0026_15_01_1999.html>. [Accessed 29 July 2020].
35. Ministério da Saúde. (2006). *VIGILÂNCIA E CONTROLE DA QUALIDADE DA ÁGUA PARA CONSUMO HUMANO*. [online]. Available at: https://bvsms.saude.gov.br/bvs/publicacoes/vigilancia_controle_qualidade_agua.pdf>. [Accessed 29 July 2020].
36. Nunes LGDP, Oliveira MDV, de Souza AA, Lopes LDF, Dias PCES, Nogueira GB, Souza MAAD (2018) Water quality comparison between a supply network and household reservoirs in one of the oldest cities in Brazil. *Int J Environ Health Res* 29(2):173–180. <https://doi.org/10.1080/09603123.2018.1531114>

37. Pacheco MH, Esmerino EA, Capobiango CS, Cruz AG, Leddomado LS, Pimentel TC, de Freitas MQ (2018) Bottled mineral water: classic and temporal descriptive sensory analysis associated with liking. *British Food Journal* 120(7):1547–1560. <https://doi.org/10.1108/BFJ-11-2017-0655>
38. Pazand K, Khosravi D, Ghaderi MR, Rezvanianzadeh MR (2018) Identification of the hydrogeochemical processes and assessment of groundwater in a semi-arid region using major ion chemistry: A case study of Ardestan basin in Central Iran. *Groundwater for Sustainable Development* 6:245–254. <https://doi.org/10.1016/j.gsd.2018.01.008>
39. Piper AM (1944) A graphic procedure in the geochemical interpretation of water-analyses. *Eos, Transactions American Geophysical Union* 25(6):914–928. <https://doi.org/10.1029/TR025i006p00914>
40. R Core Team (2019) R: A language and environment for statistical computing. R Foundation for Statistical Computing
41. Sargazi S, Mokhtari M, Ehrampoush MH, Almodaresi SA, Sargazi H, Sarhadi M (2020) The application of geographical information system (GIS) approach for assessment of groundwater quality of Zahedan city, Sistan and Baluchestan Province, Iran. *Groundwater for Sustainable Development* 100509. <https://doi.org/10.1016/j.gsd.2020.100509>
42. Schwanz TG, Llorca M, Farré M, Barceló D (2016) Perfluoroalkyl substances assessment in drinking waters from Brazil, France and Spain. *Sci Total Environ* 539:143–152. <https://doi.org/10.1016/j.scitotenv.2015.08.034>
43. Shruti VC, Pérez-Guevara F, Kutralam-Muniasamy G (2020) Metro station free drinking water fountain- A potential “microplastics hotspot” for human consumption. *Environ Pollut* 261:114227. <https://doi.org/10.1016/j.envpol.2020.114227>
44. Silva TA, Rosário FF, Silva Júnior GC (2020) Environmental isotopes and hydrochemical tracers applied to hydrogeological conceptual modeling of the southwest portion of the Amazon Aquifer System (Acre, Brazil). *Appl Geochem* 120:104670. <https://doi.org/10.1016/j.apgeochem.2020.104670>
45. Teramoto EH, Gonçalves RD, Chang HK (2020) Hydrochemistry of the Guarani Aquifer System modulated by mixing with underlying and overlying hydrostratigraphic units. *Journal of Hydrology: Regional Studies* 30:100713. <https://doi.org/10.1016/j.ejrh.2020.100713>
46. Tiwari K, Goyal R, Sarkar A (2017) GIS-based spatial distribution of groundwater quality and regional suitability evaluation for drinking water. *Environmental Processes* 4(3):645–662. <https://doi.org/10.1007/s40710-017-0257-4>
47. Tlili-Zrelli B, Gueddari M, Bouhlila R, Naceur M, O (2015) Groundwater hydrogeochemistry of Mateur alluvial aquifer (Northern Tunisia). *J Hydrogeol Hydrol Eng* 5(1). <http://dx.doi.org/10.4172/2325-9647.1000128>
48. Tundisi JG (2008) Water resources in the future: problems and solutions. *Estudos avançados* 22(63):7–16. <https://doi.org/10.1590/S0103-40142008000200002>

49. Vauclin M, Vieira SR, Vachaud G, Nielsen DR (1983) The Use of Cokriging with Limited Field Soil Observations 1. *Soil Sci Soc Am J* 47(2):175–184. 10.2136/sssaj1983.03615995004700020001x
50. Warrick AW, Nielsen DR (1980) Spatial variability of soil physical properties in the field.. In: In: HILLEL D (ed) *Applications of Soil Physics*, vol 2. Academic, New York, pp 319–344
51. Yang Q, Li Z, Ma H, Wang L, Martín JD (2016) Identification of the hydrogeochemical processes and assessment of groundwater quality using classic integrated geochemical methods in the Southeastern part of Ordos basin, China. *Environ Pollut* 218:879–888. <https://doi.org/10.1016/j.envpol.2016.08.017>
52. Yang Q, Li Z, Ma H, Wang L, Martín JD (2016) Identification of the hydrogeochemical processes and assessment of groundwater quality using classic integrated geochemical methods in the Southeastern part of Ordos basin, China. *Environ Pollut* 218:879–888. <https://doi.org/10.1016/j.envpol.2016.08.017>
53. Yang Q, Li Z, Xie C, Liang J, Ma H (2020) Risk assessment of groundwater hydrochemistry for irrigation suitability in Ordos Basin, China. *Nat Hazards* 101:309–325. <https://doi.org/10.1007/s11069-018-3451-4>
54. Yin S, Xiao Y, Gu X, Hao Q, Liu H, Hao Z, Pei Q (2019) Geostatistical analysis of hydrochemical variations and nitrate pollution causes of groundwater in an alluvial fan plain. *Acta Geophys* 67(4):1191–1203. <https://doi.org/10.1007/s11600-019-00302-5>
55. Yin, S., Xiao, Y., Gu, X., Hao, Q., Liu, H., Hao, Z., ... & Pei, Q. (2019). Geostatistical analysis of hydrochemical variations and nitrate pollution causes of groundwater in an alluvial fan plain. *Acta Geophysica*, 67(4), 1191-1203. <https://doi.org/10.1007/s11600-019-00302-5>

Figures

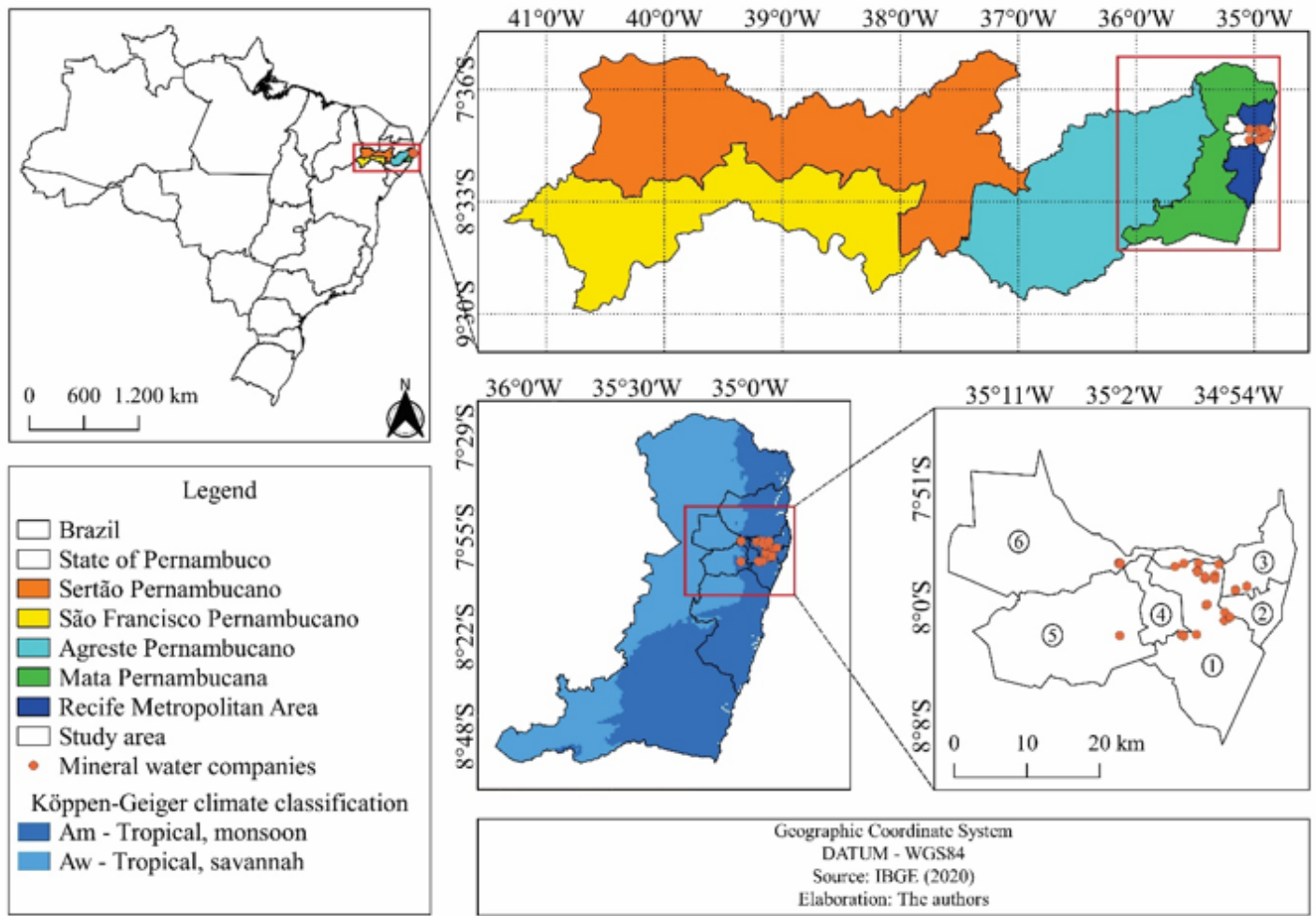


Figure 1

Spatial map of location of the study area, municipalities of Recife (1), Olinda (2), Paulista (3), Camaragibe (4), São Lourenço da Mata (5), and Paudalho (6) and distribution of sampling points.

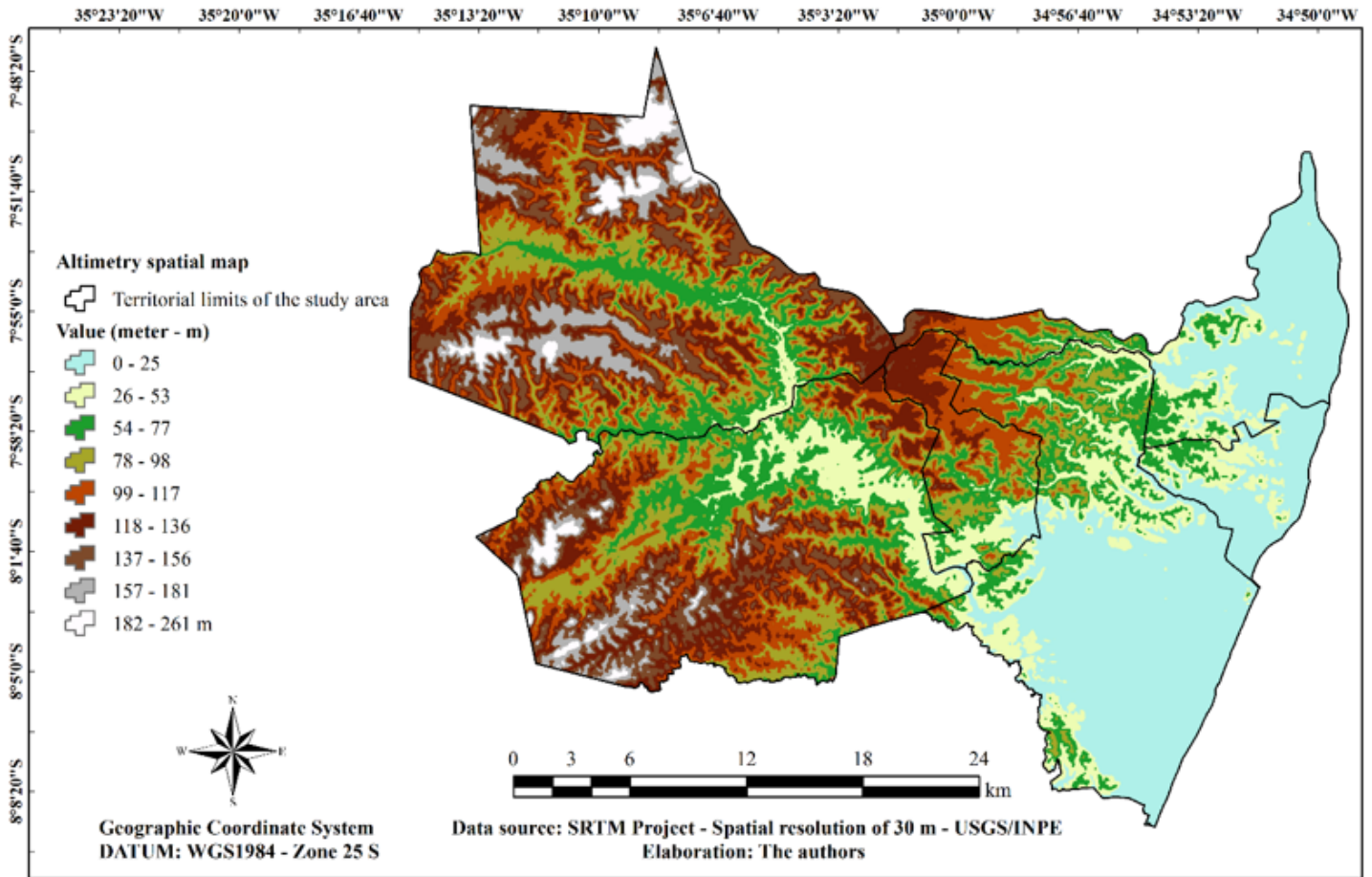


Figure 2

Spatial altimetry (m) map of the study area, cities of Recife, Olinda, Paulista, Camaragibe, São Lourenço da Mata and Paudalho.

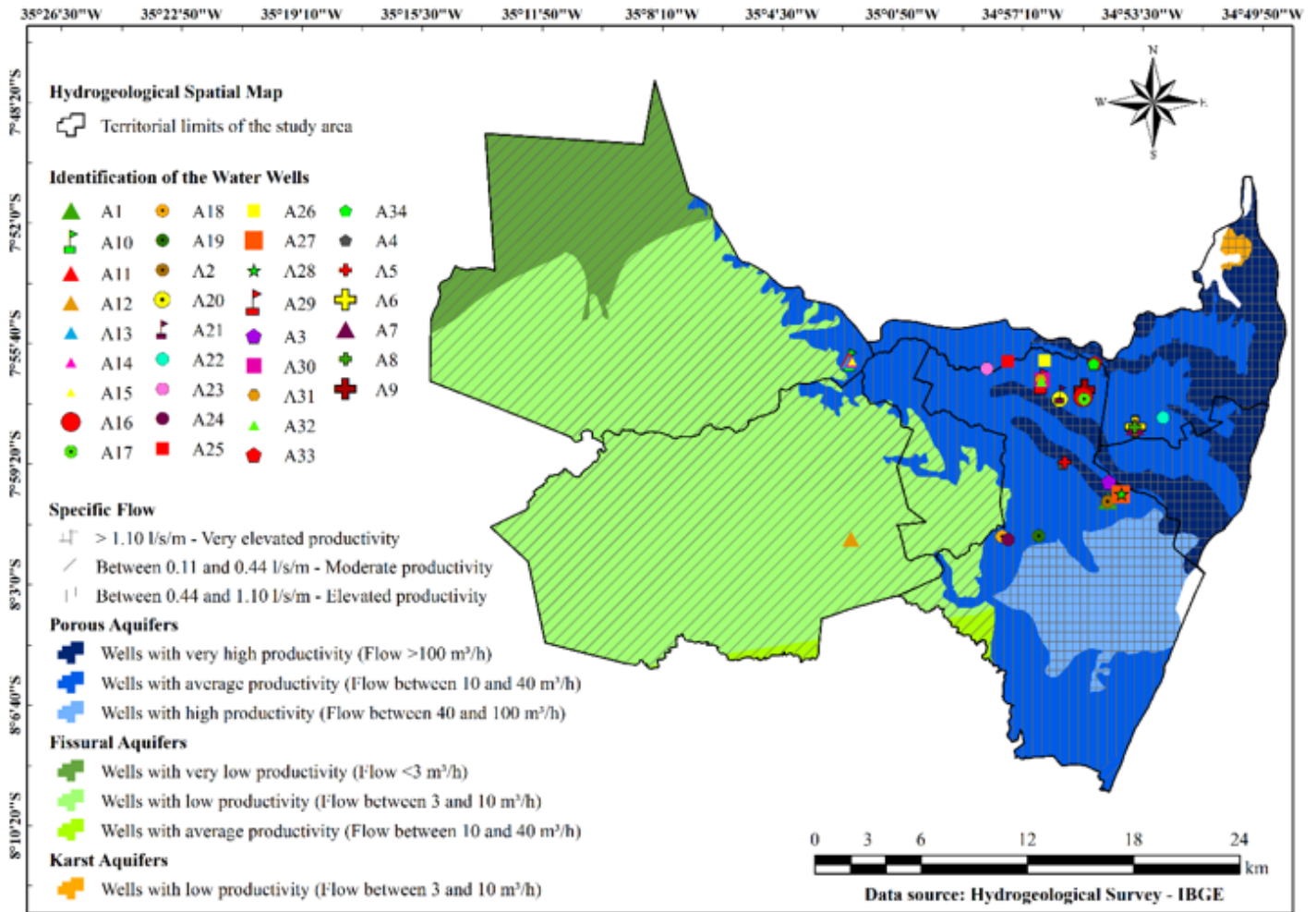


Figure 3

Spatial map of the hydrogeological characterization of the groundwater of the Beberibe aquifer in the study area, cities of Recife, Olinda, Paulista, Camaragibe, São Lourenço da Mata, and Paudalho, and distribution of the sampling points.

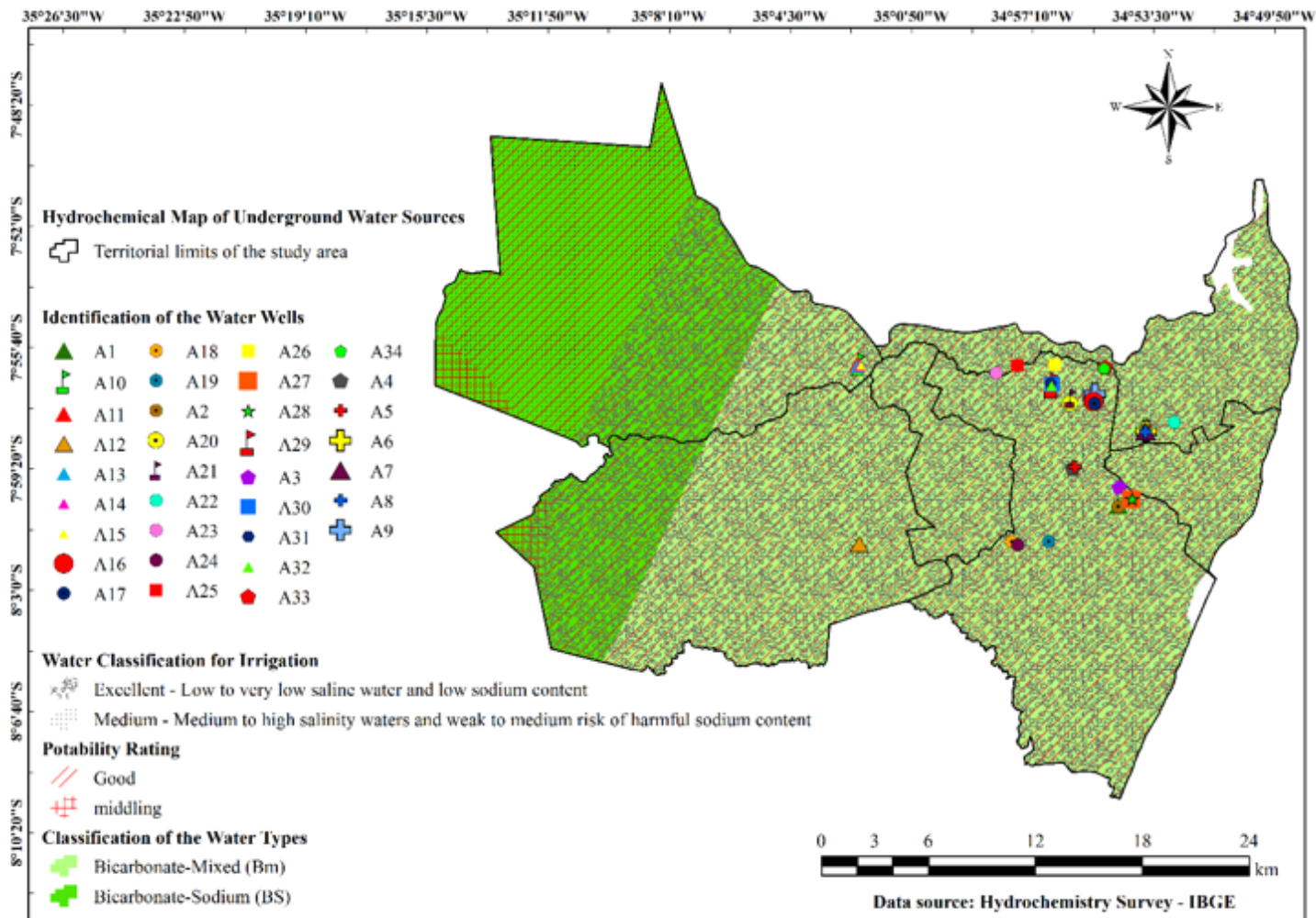


Figure 4

Hydrochemical spatial map of the groundwater of the Beberibe aquifer in the study area, municipalities of Recife, Olinda, Paulista, Camaragibe, São Lourenço da Mata, and Paudalho, and distribution of the sampling points.

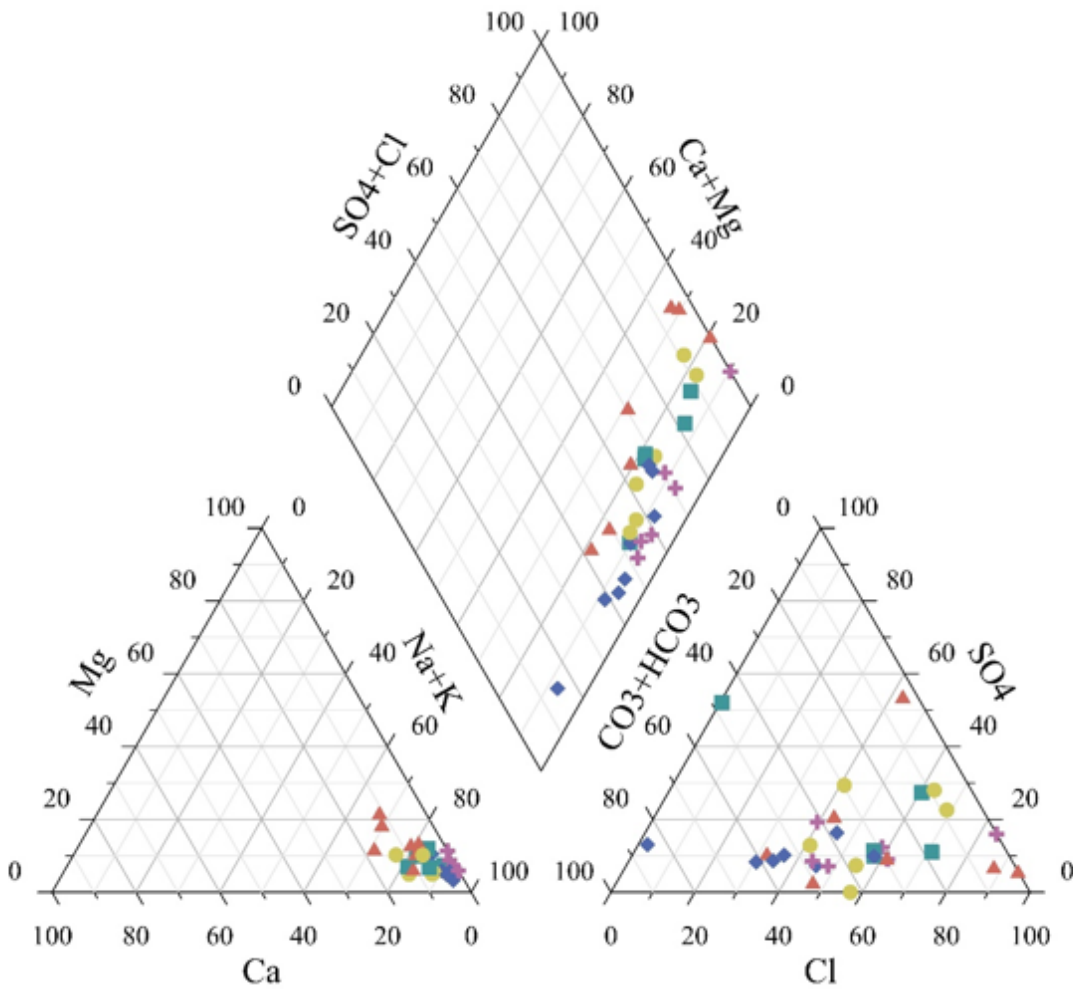


Figure 5

Piper's diagram of the hydrochemical parameters of the mineral water of the Beberibe aquifer in the study area.

Figure 6

Spatial distribution of the hydrochemical parameters of the mineral water from the Beberibe aquifer in the study area.

NO₃: Nitrate; DR: Evaporative resistance; pH: Hydrogen potential; SO₄: Sulfate; Na: Sodium; Ca: Calcium; Mg: Magnesium; Cl: Chlorine; K: Potassium; Mn: Manganese; F: Fluorine; Zn: Zinc; Fe: Iron; EC: Electrical conductivity; Hn: Hardness; HCO₃: Bicarbonate; Si: Silicon; Sr: Strontium; Ba: Barium.

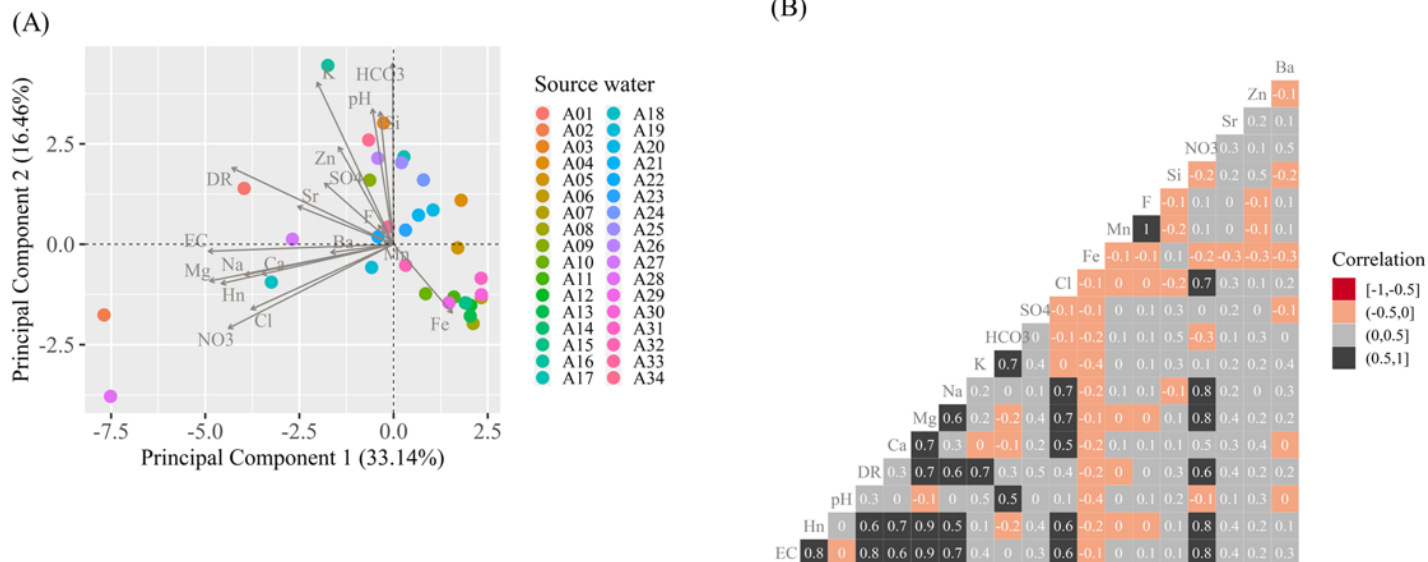


Figure 7

Biplot plot of the principal components (A) and Pearson's correlation (B) of the hydrochemical parameters of the mineral water of the Beberibe aquifer in the study area.

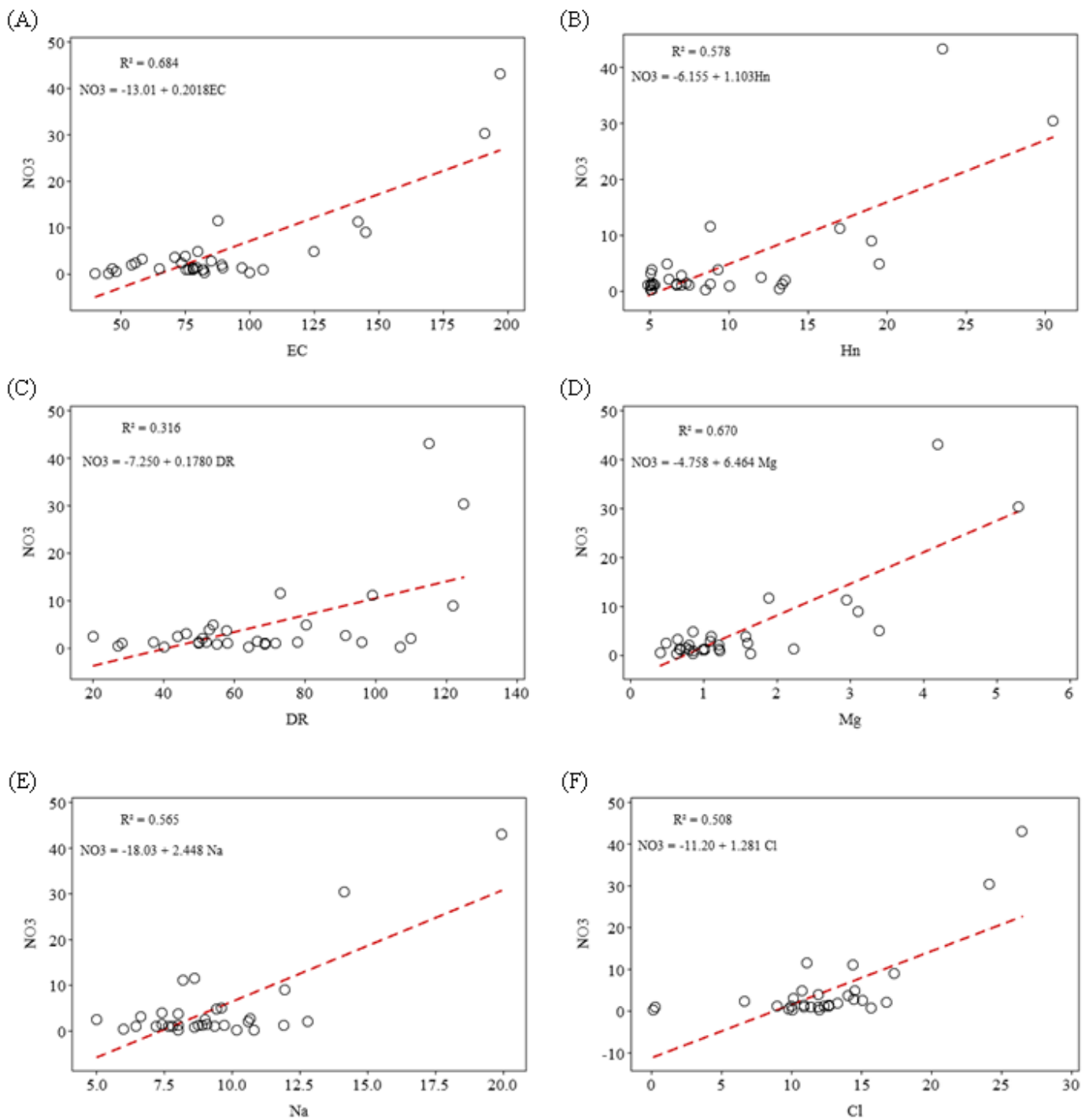


Figure 8

Linear regression models for the variables with the highest correlation with nitrate (NO_3); NO_3 x electrical conductivity (EC) (A); NO_3 x hardness (Hn) (B); NO_3 x evaporative resistance (DR) (C); NO_3 x magnesium (Mg) (D); NO_3 x sodium (Na) (E); NO_3 x chlorine (Cl) (F).